

# Atomistic simulation on the time development of coarse-grained structure of inorganic material

Hiroshi Ogawa

National Institute of Advanced Industrial Science and Technology (AIST),  
1-1, Umezono, Tsukuba, 305-8568, Japan.  
FAX: 81-29-861-3171, e-mail: h.ogawa@aist.go.jp

A molecular dynamics simulation was carried out to investigate the grain growth phenomenon and grain boundary structures in metallic polycrystals at high temperature. The initial structures were composed of 64 grains of bcc-Fe of which crystal orientations were randomly selected by assuming three different co-rotation axes. Grain growths satisfying the parabolic law were successfully reproduced. Crystal orientations and boundary misorientation angles were analyzed at initial, middle and last stages of the grain growth. CSL boundaries with low  $\Sigma$  values were spontaneously generated during the grain growth in the samples with  $\langle 100 \rangle$  and  $\langle 311 \rangle$  co-rotation axes. Random-like boundaries were generated in a sample with  $\langle 753 \rangle$  co-rotation axis. Low-angle boundaries were relatively few in all simulated samples.

Key words: molecular dynamics, grain growth, grain boundary, CSL boundary

## 1. INTRODUCTION

Understanding the microstructures and textures in polycrystals is important for improving the inorganic material properties. Because the formation of microstructures usually occurs at high temperatures, in-situ observation of formation process is quite difficult. Computer simulation is helpful for understanding what happens in materials. The mean field theory,<sup>1,2)</sup> Monte Carlo method,<sup>3)</sup> vertex model,<sup>4)</sup> and surface evolver method<sup>5)</sup> were applied to microstructure formation and grain growth processes in polycrystals. Most of these studies, however, frequently neglected the atomistic structure in grains and grain boundaries and hence were limited to an isotropic medium.

In actual polycrystalline materials, atomistic structures are known to play important roles. Grain boundaries are classified into several types: tilt, twist, coincident, random, etc. Such complexity in grain boundary structures is originated to the large degree of freedom on the geometrical arrangement of neighboring crystals. Five angles are known to be required for describing the grain boundary geometry,<sup>6)</sup> two of them are indices for the orientation of the interface and the rest three are the misorientation angles. In the atomistic level, further three (if the vertical position of boundary is included, four) translative values must be taken into account. Physical properties of a grain boundary, and hence also the macroscopic properties of polycrystals are strongly dependent on grain boundary geometry.<sup>7)</sup>

Using an atomistic simulation method is essential for reproducing such characteristics of microscopic polycrystalline structures. The present author used the molecular dynamics (MD) method

for simulating metallic nanocrystals and successfully reproduced the grain growth phenomena in atomistic levels.<sup>8,9)</sup> In the present study, the author again uses the MD method to analyze the grain boundary characteristics for several different initial conditions.

## 2. SIMULATION

Three-dimensional polycrystalline models were constructed by weighted-Voronoi partitioning<sup>9)</sup> of the rectangular MD cell of which size is about  $25 \times 25 \times 1.5 \text{ nm}^3$ . Initially, 64 grains with different crystal orientations were generated in the MD cell. In order to avoid the surface effects, three-dimensional periodic boundary conditions were applied to the MD cell. So as to eliminate the grain boundaries normal to the z direction, crystal orientations of the grains were limited to be described by one co-rotation axis and one rotation angle. Hence, all grains have an infinite length toward z direction, and all grain boundaries are parallel to z axis and tilt type.

The target material of the present study is bcc-Fe polycrystals. Three different Miller indices,  $\langle 110 \rangle$ ,  $\langle 311 \rangle$  and  $\langle 753 \rangle$ , were assumed for the co-rotation axis. The rotation angles of grains in initial configurations were selected at random. By changing the grain positions, radii, and rotation angles, 8 different models were generated for each co-rotation axis, hence 24 different initial configurations were used for the simulation.

The MD simulation was carried out using the interatomic potential proposed by Finnis and Sinclair.<sup>10)</sup> The simulation started by a short relaxation process at the room temperature. After elevating temperature to 1680 K, constant NPT

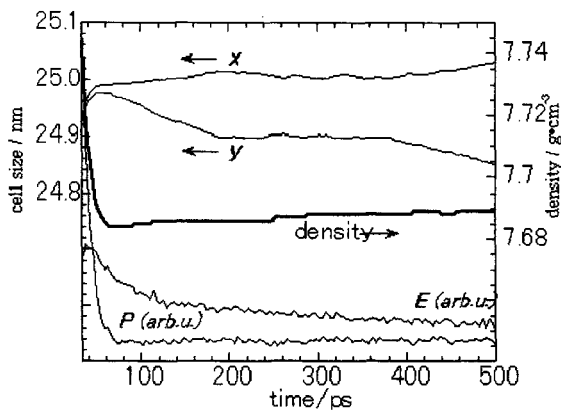


Fig. 1 Time variation of the system size ( $x$ ,  $y$ ), density, total energy ( $E$ ) and total pressure ( $P$ ) of a  $\langle 311 \rangle$  sample.

simulation was carried out until the number of grains reduces to less than 4 (up to about 1 ns). The simulation was carried out on the PC clusters, HIT HPC-HP2SC/Myrinet and IAX/TA5/Mini Cube. Misorientation angles of coincident site lattice (CSL) boundaries were analyzed by using the software "GBstudio".<sup>11)</sup>

### 3. RESULTS AND DISCUSSION

Because the initial structure involves a large volume fraction of boundary regions, significant structural relaxation occurred at the beginning of the simulation. Figure 1 shows the time variations of the system sizes, density, total energy and total pressure of a sample with  $\langle 311 \rangle$  co-rotation axis. At the first stage of the simulation until about 60 ps, the sample quickly expanded so as to release the high pressure caused by the precedent heating process. Time variations after the pressure relaxation are considered to be caused by the grain growth

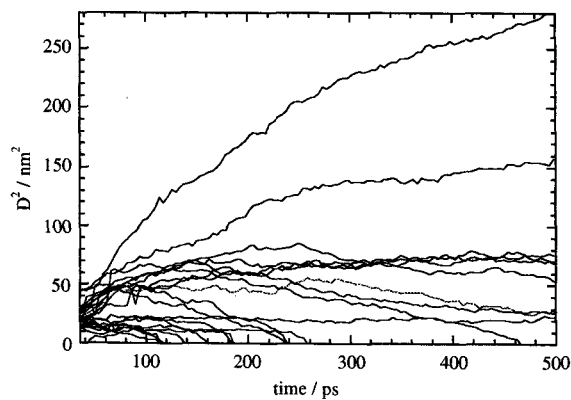


Fig. 2 Time variations of the diameters of several grains in a  $\langle 311 \rangle$  sample.

phenomenon. During the grain growth, the total energy gradually decreases and the density increases due to the reduction of grain boundary regions.

The number of grains reduced to 50 and 20 by roughly 200 and 500 ps, respectively. Time variations of the diameters  $D$  of individual grains are plotted in Fig. 2. Generally speaking, relatively small grains tend to shrink and large ones grow at each stage of the grain growth. As the result, the number of grains decreases monotonously with time, and hence the mean radius of grains increases. The growth curve of the averaged grain size was in good agreement with the parabolic law<sup>12)</sup> as shown elsewhere.<sup>8)</sup>

Figure 3 shows the time variations of diameter and crystal orientation of a specified grain. It is known that the crystal orientation is not fixed during the grain growth but varies by several degrees. In the case of the exemplified grain, variation of crystal orientation temporarily stopped at about 200 ps just before the diameter started to increase. After the diameter reached to the maximum value, variations of both diameter and orientation started again. Such correlational variation between grain size and crystal orientation is considered to be caused by the interactions with surrounding grains.

If a misorientation angle between neighboring grains satisfies the CSL condition, the grain boundary energy decreases drastically.<sup>13)</sup> Such coincident boundaries were found in the present simulation. Figure 4 shows the distribution of the misorientation angles of the simulated grain boundaries at initial, middle and last stages of the grain growth in two samples with  $\langle 110 \rangle$  co-rotation axis. The angular distribution at the initial stage is relatively homogeneous since the initial grain orientations were selected at random. At the middle and last stages of the grain growth, however, dominant peaks at  $70.5^\circ$  were observed in both cases. By the CSL theory, these peaks are attributed to  $\Sigma 3$  boundaries.

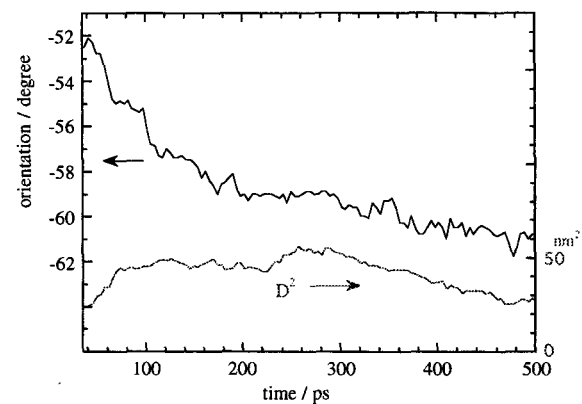


Fig. 3 Time variations of the mean diameter and crystal orientation of a selected grain in a  $\langle 311 \rangle$  sample.

Wolf<sup>43)</sup> reported that the  $\Sigma 3$  symmetrical tilt boundary with (112) plane has a lowest boundary energy in  $\langle 110 \rangle$  rotations. Other peaks in the figure, however, cannot be well assigned to low  $\Sigma$  boundaries. In both samples, low-angle boundaries with misorientation angles less than  $15^\circ$  were found to be not dominant.

Simulated distribution of misorientation angle is strongly dependent on the choice of the co-rotation axis. Figure 5 shows the same results to Fig. 4 but for  $\langle 311 \rangle$  and  $\langle 753 \rangle$  co-rotation axes. Two dominant peaks at  $146.4^\circ$  and  $67.1^\circ$  in the  $\langle 311 \rangle$  sample were assigned to  $\Sigma 3$  and  $\Sigma 9$  boundaries, respectively, by investigating the misorientation angle of CSL boundaries for these axes.<sup>11)</sup> In the case of  $\langle 753 \rangle$  sample, the lowest  $\Sigma$  boundary is  $\Sigma 21b$  at  $167.5^\circ$  and was not found in the simulated sample. By these results, it is considered that the misorientation angle distribution during the grain growth process is not at random, but is adjusted so as to reduce the grain boundary energy by grain rotations as shown in Fig. 3.

#### 4. SUMMARY

The present study reveals that the formation of

microstructures in polycrystals concerning to the grain growth phenomenon can be successfully simulated by the MD method. If we use an appropriate interatomic potentials, and hence the geometrical dependences of the boundary energy are precisely taken into account, we will be able to reproduce the grain boundary characteristics in desired materials. In the present study, low  $\Sigma$  boundaries such as  $\Sigma 3$  and  $\Sigma 9$  were spontaneously generated in the grain growth process. In conclusion, the present author stresses that the MD method is useful to investigate and understand the microstructures in polycrystalline materials.

#### References

1. M. Hillert, *Acta metall.*, 13, 227-38 (1965).
2. N. P. Louat, *Acta metall.*, 22, 721-4 (1974).
3. D. J. Srolovitz, M. P. Anderson, P. S. Sahni and G. S. Grest, *Acta metall.*, 32, 793-802 (1984).
4. T. Nagai, K. Kawasaki and K. Nakamura, *J. Phys. Soc. Jpn.*, 57, 2221-4 (1988).
5. F. Wakai, N. Enomoto and H. Ogawa: *Acta Mater.*, 48, 1297-1311 (2000).
6. C. Goux, *Can. Metall. Q.*, 13, 9 (1974).

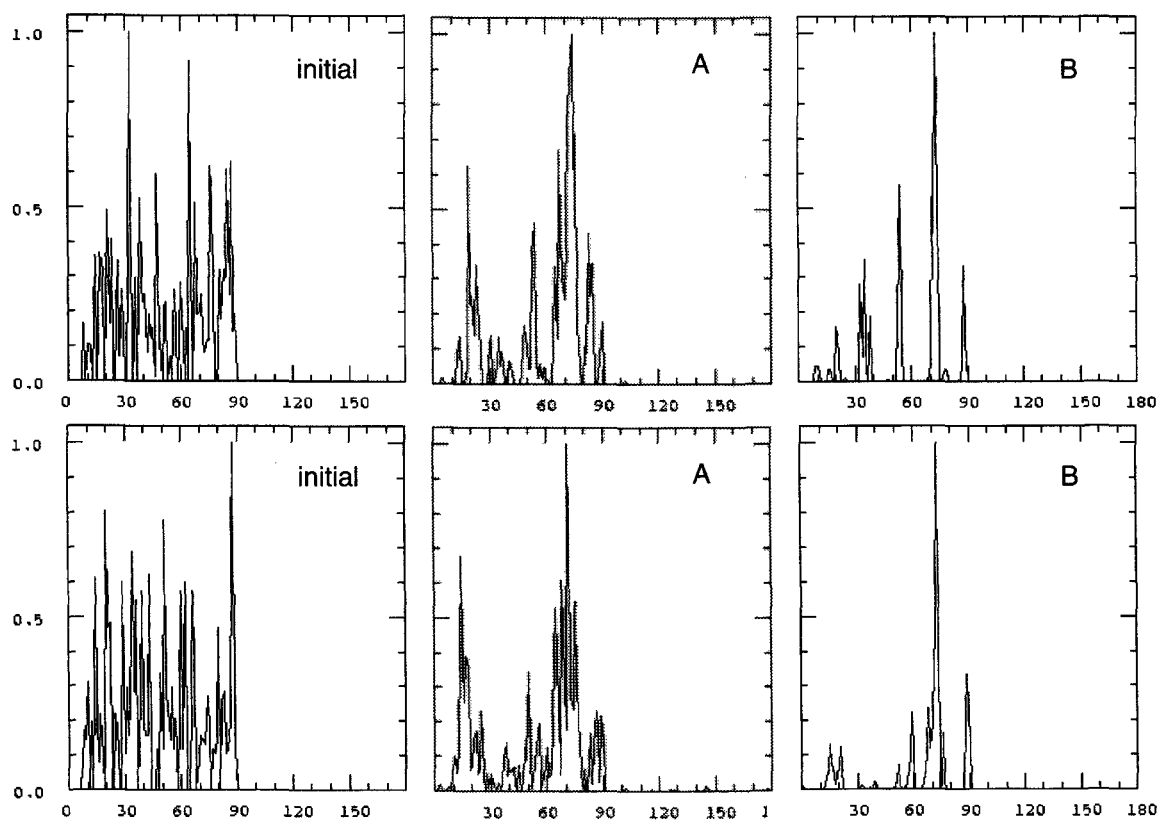


Fig. 4 Two example of the misorientation angle distribution at the initial, middle (A) and last (B) stages of the grain growths in two  $\langle 311 \rangle$  samples.

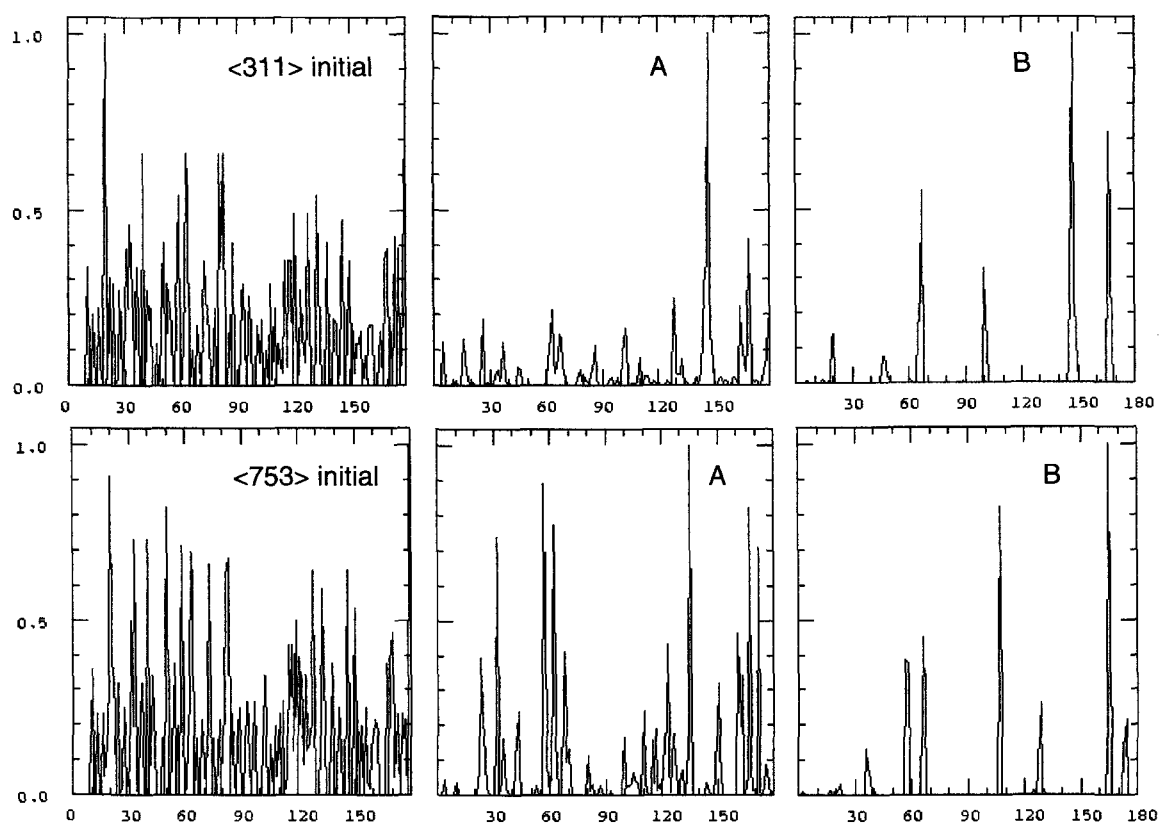


Fig. 5 Same as Fig. 4 but in  $\langle 311 \rangle$  (top) and  $\langle 753 \rangle$  (bottom) samples.

7. Special issue on grain boundaries, *J. Metals*, 50 (2) (1998).
8. H. Ogawa and F. Wakai, *Mater. Trans.*, 42, 2266–2269 (2001).
9. H. Ogawa and F. Wakai, *Mater. Res. Soc. Japan*, 27, 317–319 (2002).
10. M. W. Finnis and J.E. Sinclair, *Phil. Mag. A*, 50, 45–55 (1984).
11. H. Ogawa, "GBstudio", <http://unit.aist.go.jp/rics/soft/GBstudio/>, (2003).
12. H. V. Atkinson, *Acta metall.*, 36, 469–91 (1988).
13. D. Wolf, *Phil. Mag. A*, 62, 447–464 (1990).

(Received October 13, 2003; Accepted March 17, 2004)